Role of limiting dispersal on metacommunity stability and persistence

Snehasish Roy Chowdhury,[1] Ramesh Arumugam,[1,*] Wei Zou,[2] V. K. Chandrasekar,[3,†] and D. V. Senthilkumar[1,‡]

[1]*School of Physics, Indian Institute of Science Education and Research, Thiruvananthapuram 695551, Kerala, India*

[2]*School of Mathematical Sciences, South China Normal University, Guangzhou 510631, People's Republic of China*

[3]*Department of Physics, Centre for Nonlinear Science and Engineering, School of Electrical and Electronics Engineering, SASTRA Deemed University, Thanjavur 613401, Tamilnadu, India*

(Received 27 July 2021; revised 15 November 2021; accepted 1 March 2022; published 23 March 2022)

The role of dispersal on the stability and synchrony of a metacommunity is a topic of considerable interest in theoretical ecology. Dispersal is known to promote both synchrony, which enhances the likelihood of extinction, and spatial heterogeneity, which favors the persistence of the population. Several efforts have been made to understand the effect of diverse variants of dispersal in the spatially distributed ecological community. Despite that environmental change strongly affects the dispersal, the effects of controlled dispersal on the metacommunity stability and their persistence remain unknown. We study the influence of limiting the immigration using two-patch prey-predator metacommunity at both local and spatial scales. We find that the spread of the inhomogeneous stable steady states (asynchronous states) decreases monotonically upon limiting the predator dispersal. Nevertheless, at the local scale, the spread of the inhomogeneous steady states increases up to a critical value of the limiting factor, favoring the metacommunity persistence, and then starts decreasing for a further decrease in the limiting factor with varying local interaction. Interestingly, limiting the prey dispersal promotes inhomogeneous steady states in a large region of the parameter space, thereby increasing the metacommunity persistence at both spatial and local scales. Further, we show similar qualitative dynamics in an entire class of complex networks consisting of a large number of patches. We also deduce various bifurcation curves and stability conditions for the inhomogeneous steady states, which we find to agree well with the simulation results. Thus, our findings on the effect of the limiting dispersal can help to develop conservation measures for ecological communities.

DOI: 10.1103/PhysRevE.105.034309

I. INTRODUCTION

Synchrony, referring to the coherent behavior of coupled systems [1], has been studied extensively in numerous fields, such as neuroscience, physiology, biology, ecology [2–4], etc. In population dynamics, synchrony has received a great deal of attention since it can elevate a high risk of extinction [4–7]. Indeed, understanding the factors and mechanisms that generate population synchrony in ecology is of great importance for conservation and ecosystem management. Three major mechanisms of population synchrony are dispersal, environmental variation, and trophic interactions [4,8,9]. Among these, dispersal is a widely studied phenomenon in population dynamics [3,7,10,11]. Interestingly, not only can dispersal lead to synchronized behavior among the spatially distributed populations, but it can also rescue populations through recolonization [12–14]. Consequently, dispersal can also act as a stabilizing mechanism in diverse systems and has a huge impact on the persistence of ecological communities [6,15]. In this scenario, a small change or control over the dispersal can have tremendous consequences on the stability and ecosystem functioning. In this study, we present how limiting the dispersal of both predator and prey populations can affect the stability and persistence of a spatially distributed community.

Climate change affects the stability of many ecological communities by altering their dispersal pattern and the associated responses [16–19]. Major ecological responses to environmental changes include adaptation, migration, and extinction [20–24]. Species that lack the adaptation for environmental variation tend to migrate to suitable habitats. While species migrate, they can face an additional mortality due to failed migration, misdirected migration, and overcrowding [25]. Typically, species immigration is reduced by habitat loss, habitat fragmentation, and anthropogenic changes [20,21,26]. Indeed, climate change and other factors can also limit the species dispersal. In this connection, theoretical studies addressing the effect of controlled dispersal are rare. Despite a plethora of studies focused on understanding the role of dispersal on the metacommunity persistence, it remains unclear how a limited dispersal affects the metacommunity stability. Since coupled ecological oscillators constitute an efficient framework to understand the dynamical effects of dispersal, in this work we address (1) how a limited dispersal of both predator and prey populations affects the stability and persistence of a spatially distributed community and (2) how a limited dispersal along with local and spatial interactions influences the synchronized and asynchronized dynamics of the metacommunity.

*ramesha@iisertvm.ac.in
†chandru25nld@gmail.com
‡skumar@iisertvm.ac.in

 ©2022 American Physical Society

In this study, we address the dynamical effects of limiting the dispersal of a predator-prey ecological system. In particular, we investigate the metacommunity persistence using homogeneous (synchronized) and inhomogeneous (asynchronized) dynamical behavior by limiting the predator and prey dispersal. Our results reveal that a small change in the predator dispersal monotonically reduces the inhomogeneous behavior as a function of the spatial interaction (predator and prey dispersal rates). In contrast, for a varying local interaction (carrying capacity), a small decrease in the predator dispersal initially increases the inhomogeneous states up to a critical value of the limiting factor, and eventually the inhomogeneous states lose their stability resulting in a homogeneous dynamical state for further decrease in the degree of the limited dispersal. Moreover, there exists a critical value of the limiting factor below which the metacommunity persists and above which the metacommunity has a risk of extinction. On the other hand, limiting the prey dispersal manifests the stable inhomogeneous steady states in a large region of the parameter space, thereby increasing the metacommunity persistence. We also consider an entire class of complex networks of metacommunity to corroborate robustness of the results. We also determine transcritical and Hopf bifurcation curves along with stability condition for the inhomogeneous steady state for a possible case. We find that the stability condition agrees well with the simulation results. This study reveals that a controlled dispersal strongly influences the metacommunity persistence by altering the asynchronized dynamics.

We organize the paper as follows. In the Models and Methods section, we describe a two-patch predator-prey metacommunity model with limiting factors in the diffusive coupling. In the Results section, we present the effect of limited predator and prey dispersal using local and spatial interactions. We also deduce the stability condition for the inhomogeneous steady (asynchronized alternative) states for the possible scenario. Subsequently, we elucidate the existence of a critical value of the limited dispersal influencing the synchronized behavior. Further, we extend our analysis to the entire class of complex networks of metacommunity to generalize our results. Finally, we discuss the ecological significance of our findings in the Discussion section.

II. MODELS AND METHODS

A. A metacommunity model

We use the well-known Rosenzweig-MacArthur model [27] to represent the prey-predator dynamics in each patch, where the prey experiences logistic growth and the predator exhibits a Holling type II functional response. We consider two identical patches with diffusive coupling between them, whose governing equation is represented as

$$\frac{dV_i}{dt} = rV_i\Big(1 - \frac{V_i}{k}\Big) - \frac{aV_i}{V_i + b}H_i + d_v(\beta V_j - V_i), \quad (1a)$$

$$\frac{dH_i}{dt} = \frac{caV_i}{V_i + b}H_i - mH_i + d_h(\alpha H_j - H_i), \quad (1b)$$

where $i, j = 1, 2$ denote the patch number and $i \neq j$. V_i and H_i are the prey and predator population densities, respectively. The parameter r denotes the intrinsic growth rate, k denotes the carrying capacity, and a and c denote the maximum predation rate and predator efficiency, respectively. A half-saturation constant is denoted by b and the mortality rate of the predator by m. These parameters determine the local dynamics of the prey and the predator in a given patch. The spatial interactions of the prey and predator between two patches are determined by the prey dispersal rate d_v, predator dispersal rate d_h, and the limiting factors α and β. Dispersal between the patches is controlled by the limiting factors, which can be decreased from 1 to zero. For $\alpha = \beta = 1$, the coupling is the usual diffusive coupling widely employed in population ecology [7,11]. $\alpha < 1$ accounts for the limited predator dispersal by reducing the immigration of the predator from patch j to patch i, while $\beta < 1$ accounts for the limited prey dispersal by reducing the immigration of the prey from patch j to patch i. Note that the coupled Rosenzweig-MacArthur model with $\alpha = \beta = 1$ has been widely employed to understand the intriguing collective dynamical behaviors under various coupling scenarios [28–31]. In particular, the coexistence of a spatially synchronized state and death state, leading to chimeralike state, has been reported in a nonlocally coupled Rosenzweig-MacArthur model [28], the phenomenon of rhythmogenesis including amplitude and oscillation deaths has been reported under environmental coupling [29], the effect of the trade-off between the mismatch in the timescale of the species, dispersal, and external force on the collective dynamics has been reported in the diffusively coupled Rosenzweig-MacArthur model [30], and the effect of prey-predator dispersal on the metacommunity persistence in both constant and temporally varying environment has been reported in spatially coupled Rosenzweig-MacArthur models [31].

B. Rescaled version of coupled Rosenzweig-MacArthur model

The above coupled Rosenzweig-MacArthur model with α and β limiting predator and prey dispersal rates, respectively, can also be written as a rescaled model with standard diffusive coupling represented as

$$\frac{dV_i}{dt} = r_eV_i\Big(1 - \frac{V_i}{k_e}\Big) - \frac{aV_i}{V_i + b}H_i + \epsilon_v(V_j - V_i), \quad (2a)$$

$$\frac{dH_i}{dt} = \frac{caV_i}{V_i + b}H_i - m_eH_i + \epsilon_h(H_j - H_i), \quad (2b)$$

where, $r_e = r - d_v(1 - \beta)$, $k_e = \frac{r_e}{r}k = 1 - \frac{d_v}{r}(1 - \beta)$, $\epsilon_v = d_v\beta$, $m_e = m + d_h(1 - \alpha)$, and $\epsilon_h = d_h\alpha$. Here r_e is the decreased growth rate, m_e is the increased mortality, k_e is the effective carrying capacity, and ϵ_v and ϵ_h are the rescaled coupling coefficients. Since the range of β and α lies within [1,0], $r_e \leqslant r$ and $m_e \geqslant m$, resulting in a decreased prey growth rate and increased predator death rate in the rescaled version of the coupled Rosenzweig-MacArthur model. Note that the results of both the rescaled model with standard diffusive coupling and the original Rosenzweig-MacArthur model with limiting predator and prey dispersal rates in the coupling will be very similar to each other. In other words, the exact mapping between these two models can also be interpreted as that the observed results may not be a pure manifestation of the topological features. However, we prefer to proceed

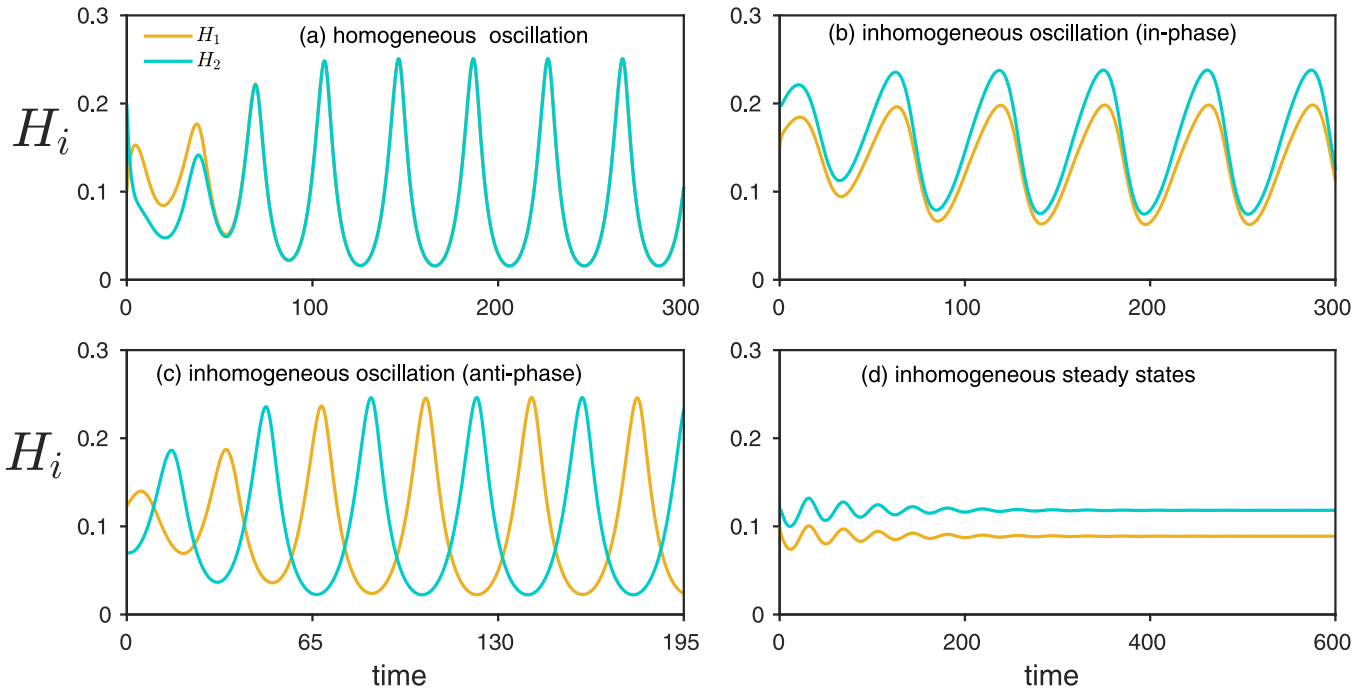

FIG. 1. Homogeneous and inhomogeneous stable states of the metacommunity model: (a) homogeneous oscillatory state for $d_h = 0.2$ and $k = 0.2$, (b) inhomogeneous oscillatory states are in in-phase for $d_h = 1$ and $k = 1.2$, (c) inhomogeneous stable oscillatory states are in antiphase for $d_h = 0.001$ and $k = 0.6$, and (d) inhomogeneous steady states for $d_h = 0.45$ and $k = 0.6$. Other parameters are $r = 0.5$, $a = 1$, $c = 0.5$, $b = 0.16$, $m = 0.2$, $d_v = 0.001$, and $\alpha = \beta = 1$.

with our analysis without rescaling the original Rosenzweig-MacArthur model but only by engineering the coupling strategies even though limiting the predator and prey dispersal rates effectively results in an increase in the predator's death rate m_e and a decrease in the prey growth rate r_e, respectively.

III. RESULTS

Before unraveling the effect of limited dispersal, we illustrate various dynamical states admitted by the metacommunity model for distinct values of the system parameters in Fig. 1. The limiting factors are fixed as $\alpha = \beta = 1$, so that the coupling is the regular diffusive coupling, which accounts for the uncontrolled dispersal [31]. We numerically integrate the governing equation of the metacommunity model using the Runge-Kutta fourth-order algorithm with a step size of $h = 0.01$. We have fixed the other parameters as $r = 0.5$, $a = 1$, $c = 0.5$, $b = 0.16$, $m = 0.2$, and $d_v = 0.001$ hereafter unless otherwise specified. Note that we have chosen the model parameters in order to get oscillatory dynamics in the uncoupled model. Indeed, the uncoupled predator-prey model exhibits the oscillatory dynamics when

$$k > \frac{b[ac + m + (1-\alpha)d_h]}{ac + (\alpha - 1)d_h - m}.$$

The model (1) exhibits similar qualitative dynamics even for other choices of the parameters. The homogeneous oscillatory state is observed for the predator dispersal rate $d_h = 0.2$ and for the carry capacity $k = 0.2$ as depicted in Fig. 1(a), which has a high probability of extinction under environmental stochasticity during the epochs of low population density. Phase synchrony (inhomogeneous oscillatory states) can be observed for $d_h = 1.0$ and $k = 1.2$ [see Fig. 1(b)], which is also prone to global extinction like the homogeneous oscillatory state in Fig. 1(a), but with a lesser probability when compared to the latter at low population density. Antiphase synchronization (inhomogeneous oscillatory states) can be observed in Fig. 1(c) for $d_h = 0.001$ and $k = 0.6$, which has a much lesser chance of extinction when compared to the homogeneous and phase-synchronized populations. One can also observe inhomogeneous steady states [see Fig. 1(d) for $d_h = 0.45$ and $k = 0.6$] of the populations, which usually coexist with homogeneous (synchronized) oscillatory state, resulting in alternative dynamical states for the population to promote their persistence.

A. Limiting predator dispersal along with spatial interaction

In this section, we will unravel the effect of limiting the predator dispersal on the dynamical transitions of the metacommunity model as a function of spatial parameters (predator and prey dispersal rates). We fix $\beta = 1$, so that the preys are allowed to disperse completely, whereas only the predator dispersal is controlled by decreasing the value of α. Bifurcation diagrams, plotted using XPPAUT [32], illustrating the dynamical transitions as a function of the predator dispersal rate are depicted in Fig. 2 for the carrying capacity $k = 0.5$. Extrema of stable homogeneous oscillatory states are plotted as filled circles, while those of unstable oscillatory states are represented by unfilled circles. Stable and unstable steady states are indicated by solid and dashed curves (lines), respectively. For $\alpha = 1$, the dispersal among the metacommunity is the usual diffusive coupling between the patches. Only stable homogeneous (synchronized) oscillation among the populations is observed all along

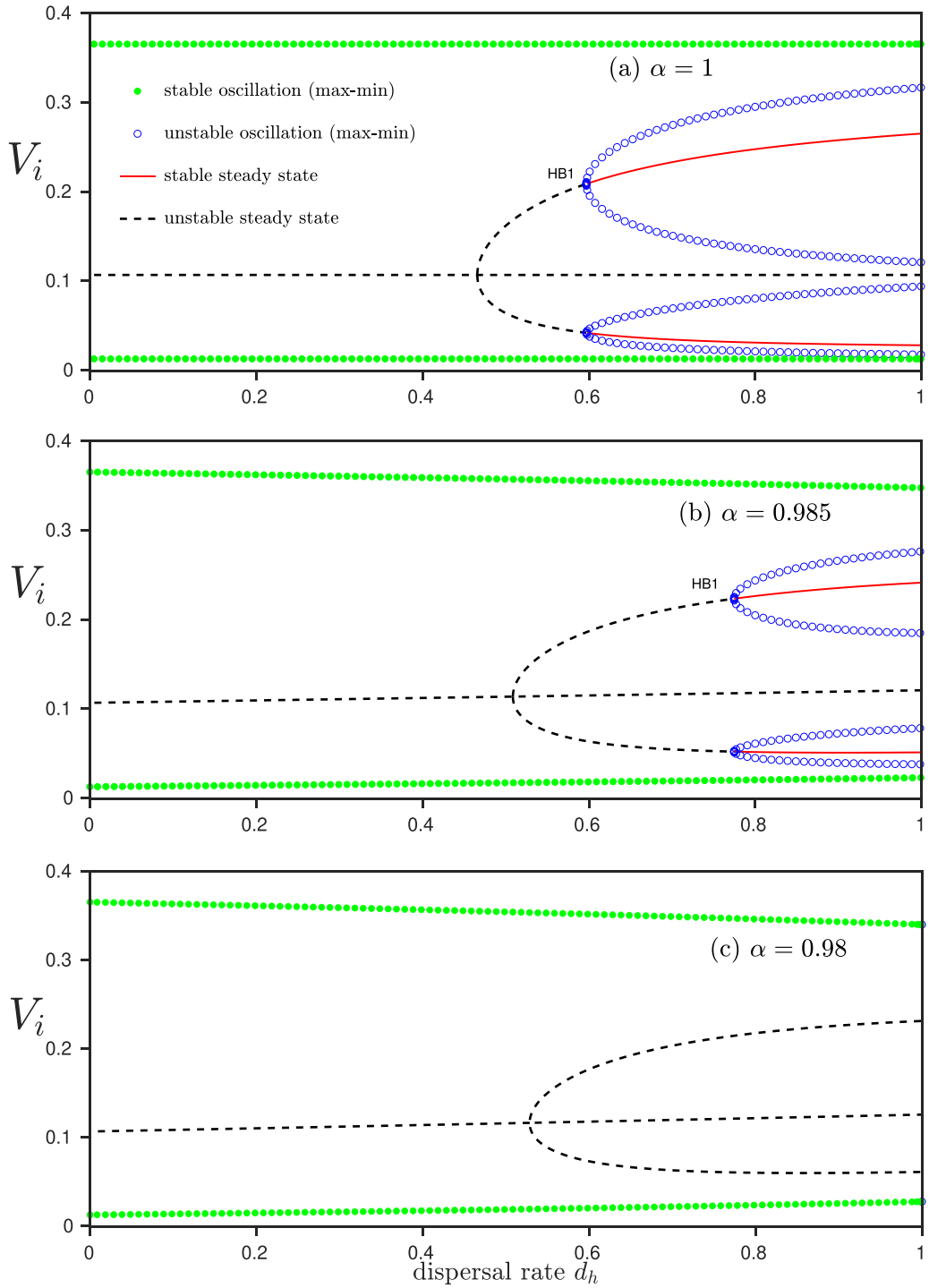

FIG. 2. Metacommunity dynamics for limiting the predator dispersal: Bifurcation diagram as a function of predator dispersal rate (d_h) is shown for different α values. Homogeneous and inhomogeneous states of the metacommunity are shown for (a) $\alpha = 1$, (b) $\alpha = 0.985$, and (c) $\alpha = 0.98$. For a small decrease in α, inhomogeneous stable steady states (red solid lines) become unstable. Here HB1 denotes Hopf bifurcation. Other parameters are $\beta = 1$, $r = 0.5$, $k = 0.5$, $a = 1$, $c = 0.5$, $b = 0.16$, $m = 0.2$, and $d_v = 0.001$

the low values of the predatory dispersal for $\alpha = 1$, where the homogeneous steady state is unstable [see Fig. 2(a)]. The former prevails in the entire explored range of the predator dispersal rate. Subcritical pitchfork bifurcation onsets at $d_h = 0.48$ resulting in the coexistence of unstable homogeneous and inhomogeneous steady states along with the homogeneous oscillatory state in the range $d_h \in [0.48, 0.597)$. A Hopf bifurcation at $d_h = 0.597$ leads to the onset of stable inhomogeneous steady (asynchronous) states, which coexist along with unstable inhomogeneous oscillatory states. The onset of the former gives rise to the emergence of alternative stable states of the populations, thereby leading to an increase in the degree of persistence of the metacommunity in the range of $d_h \in [0.597, 1.0]$.

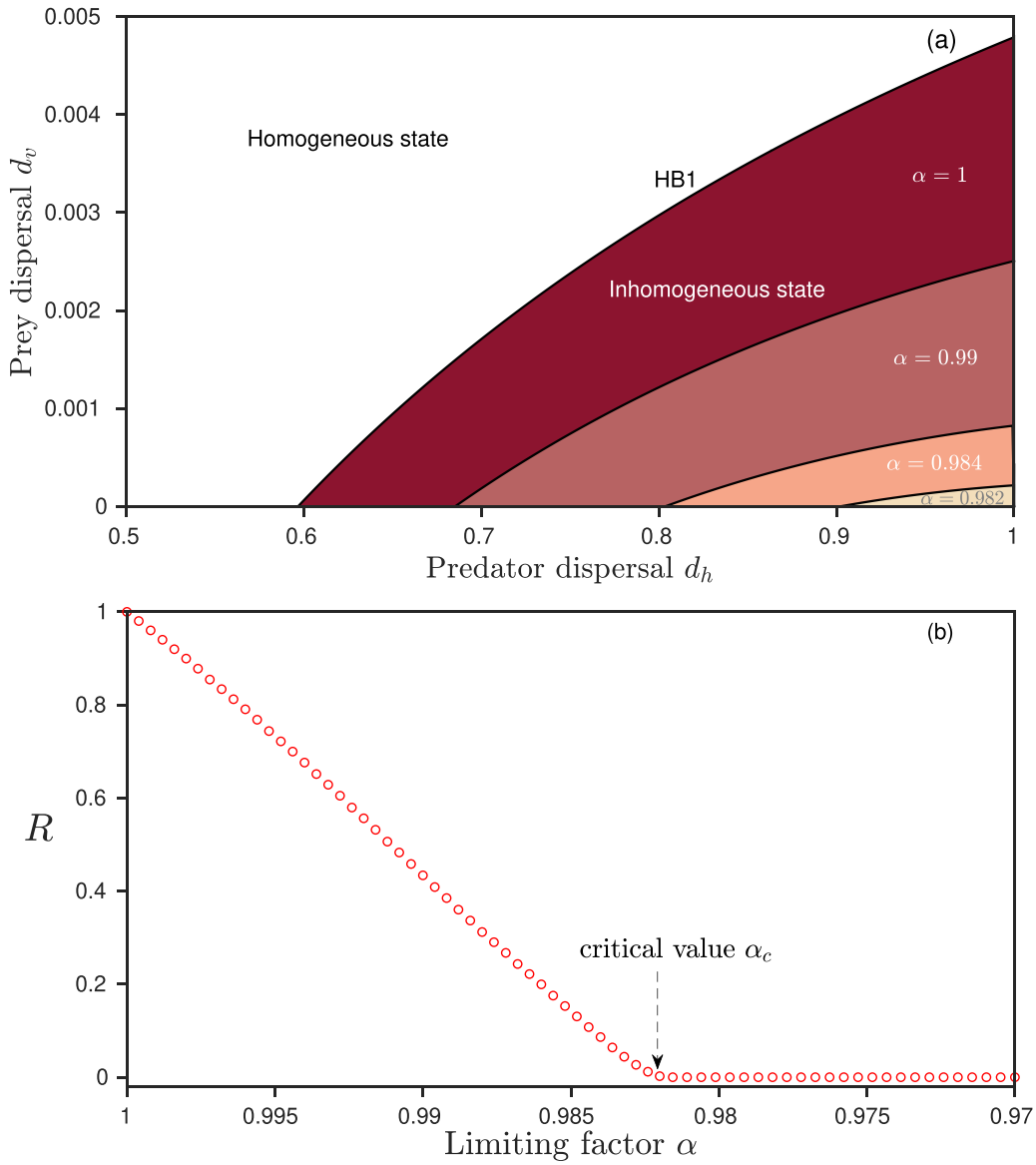

FIG. 3. (a) Two-parameter bifurcation diagram in d_h-d_v space at different α values: the Hopf bifurcation (HB1) curve separates the region into homogeneous and inhomogeneous stable states. The region below the curve indicates the spread of the inhomogeneous stable states, which decreases for decreasing α. (b) The normalized area of the spread of the stable inhomogeneous steady states defined as $R = S(\alpha)/S(\alpha = 1)$, where $S(\alpha)$ denotes the spread of the stable inhomogeneous steady states for α. Other parameter values are $\beta = 1$, $r = 0.5$, $k = 0.5$, $a = 1$, $c = 0.5$, $b = 0.16$, and $m = 0.2$.

We next control the dispersal rate of the predators using the limiting factor α and investigate the effect of limited dispersal on the metacommunity persistence. The dynamical transitions of the prey density are depicted in Fig. 2(b) for $\alpha = 0.985$. It is evident from the figure that even a feeble decrease in the limiting factor, which is a negligible fraction of decrease in dispersal, results in drastic changes in the metacommunity dynamics. The Hopf bifurcation, resulting from the onset of alternative stable states, now emerges at a higher dispersal rate at $d_h = 0.7745$ reducing the tolerance of the metacommunity persistence to a narrow range of the predator dispersal rate. This effect of limiting dispersal increases to a larger degree for further negligible decrease in the fraction of dispersal. As a consequence, the alternative stable states lose its stability in the explored range of d_h even for $\alpha = 0.98$, denoting a very small decrease in the degree of the dispersal, endangering the persistence of the metacommunity due to the presence of the homogeneous (synchronous) oscillatory state as the only dynamical state of the metacommunity, which is highly prone to extinction. In the following, we will explore the effect of controlling the predator dispersal on the metacommunity dynamics as a function of the dispersal rate of both prey and predator populations.

We have depicted the spread of the inhomogeneous steady (asynchronous, alternative) states in the two-parameter bifurcation diagram in Fig. 3(a) for a different degree of the dispersal by reducing the limiting factor α. A homogeneous oscillatory state is stable in the entire parameter space, while the inhomogeneous steady states are stable in the shaded region, where both the former and the latter coexist. The

transition from homogeneous to inhomogeneous steady state is via the Hopf bifurcation as depicted in one-parameter bifurcation diagrams in Fig. 2. Note that the Hopf bifurcation curves are obtained from XPPAUT. The spread of the inhomogeneous steady states is at a maximum for $\alpha = 1$, which monotonically decreases for a further decrease in the degree of the predator dispersal. Eventually, the inhomogeneous steady states destabilized completely in the same parameter space, where it was stable earlier, at a critical value of α resulting in the homogeneous (synchronous) oscillatory state as the only dynamical state of the metacommunity. The normalized area of the spread of the stable inhomogeneous steady states defined as $R = S(\alpha)/S(\alpha = 1)$, where $S(\alpha)$ denotes the spread of the stable inhomogeneous steady states for α, is depicted in Fig. 3(b) as a function of α. It is evident from the figure that the spread of the stable inhomogeneous steady states decreases monotonically and eventually vanishes at the critical value of $\alpha = \alpha_c \approx 0.9818$ corroborating the dynamical transitions observed in the one- and two-parameter bifurcation diagrams.

It is extremely difficult to extract the inhomogeneous steady states and deduce the stability condition analytically for finite values of prey dispersal rate d_v. However, for $d_v = 0$, the inhomogeneous steady states $(V_1^*, H_1^*, V_2^*, H_2^*)$ can be deduced as

$$V_1^* = \frac{q_1 + \sqrt{q_3 - q_1^2}}{q_2},$$

$$V_2^* = \frac{-\sqrt{q_4^2 - 4q_5(\alpha bkd_h - bkd_h - \alpha bV_1^* d_h - bkm + \alpha kV_1^* d_h - \alpha V_1^{*2} d_h)} + q_4}{2q_5},$$

$$H_1^* = -\frac{(b + V_1^*)\big(kV_1^* d_v - kV_2^* d_v - krV_1^* + rV_1^{*2}\big)}{akV_1^*},$$

$$H_2^* = -\frac{(b + V_2^*)\big(kV_2^* d_v - kV_1^* d_v - krV_2^* + rV_2^{*2}\big)}{akV_2^*},$$

where

$$q_1 = \big[d_h(2m - 2ac) + (m - ac)^2 - (\alpha^2 - 1)d_h^2\big][ack + (\alpha + 1)(b - k)d_h + m(b - k)],$$

$$q_2 = 2[ac + (\alpha - 1)d_h - m][ac - (\alpha + 1)d_h - m]^2,$$

$$q_3 = q_2[ac - (\alpha + 1)d_h - m]\{a^2c^2k^2 + 2d_h[ack(\alpha b - k) + m(b^2 + k^2)] - 2ack^2m - (\alpha^2 - 1)(b^2 + k^2)d_h^2 + m^2(b^2 + k^2)\},$$

$$q_4 = -ack - bd_h - bm + kd_h + km, \quad \text{and}$$

$$q_5 = (-ac + d_h + m).$$

The corresponding Jacobian matrix can be given as

$$A = \begin{pmatrix} -d_v + r(1 - \frac{2V_1^*}{k}) + s_1 - s_2 & -s_5 & d_v & 0 \\ cs_2 - cs_1 & cs_5 - d_h - m & 0 & \alpha d_h \\ d_v & 0 & -d_v + r(1 - \frac{2V_2^*}{k}) + s_3 - s_4 & -s_6 \\ 0 & \alpha d_h & cs_4 - cs_3 & cs_6 - d_h - m \end{pmatrix},$$

where, $s_1 = \frac{ah_1V_1^*}{(b+V_1^*)^2}$, $s_2 = \frac{ah_1}{b+V_1^*}$, $s_3 = \frac{ah_2V_2^*}{(b+V_2^*)^2}$, $s_4 = \frac{ah_2}{b+V_2^*}$, $s_5 = \frac{aV_1^*}{b+V_1^*}$, and $s_6 = \frac{aV_2^*}{b+V_2^*}$. One can deduce the characteristic equation from the Jacobian as

$$\lambda^4 - \mathrm{Tr}(A)\lambda^3 + a_2\lambda^2 - a_3\lambda + \mathrm{Det}(A) = 0. \tag{3}$$

The condition for the stability of the inhomogeneous steady (alternative) states can be obtained in terms of the system parameters as

$$F_\alpha(a, b, c, k, m, r, \alpha, d_h) = a_3[\mathrm{Tr}(A)a_2 - a_3] - \mathrm{Tr}(A)^2\mathrm{Det}(A) > 0. \tag{4}$$

The inhomogeneous steady state is stable for $F_\alpha > 0$ and unstable for $F_\alpha < 0$. $\hat{F} = F_\alpha/F_1$ is depicted in Fig. 4 as a function of the limiting factor for three predator dispersal rates $d_h = 0.8, 0.9$, and 1. The value of the limiting factor α at which $\hat{F} = 0$ corresponds to the critical value $\alpha = \alpha_c$, where there is a switch in the stability of the inhomogeneous steady state. The Hopf bifurcation curves plotted using XPPAUT in Fig. 3(a) for the critical values of the limiting factor $\alpha_c = 0.984$ and 0.982 coincide with the predator dispersal rate (x axis where $d_v = 0$) nearly at $d_h = 0.8$ and 0.9, respectively, corroborating the critical value of the limiting factor, at which there is a change in the stability of the inhomogeneous steady state, obtained using the analytical stability curve in Fig. 4.

B. Limiting predator dispersal along with local interaction

In this section, we investigate the influence of the limited predator dispersal and a local parameter (carrying capacity) on the dynamics of the metacommunity for $\beta = 1$. The predator

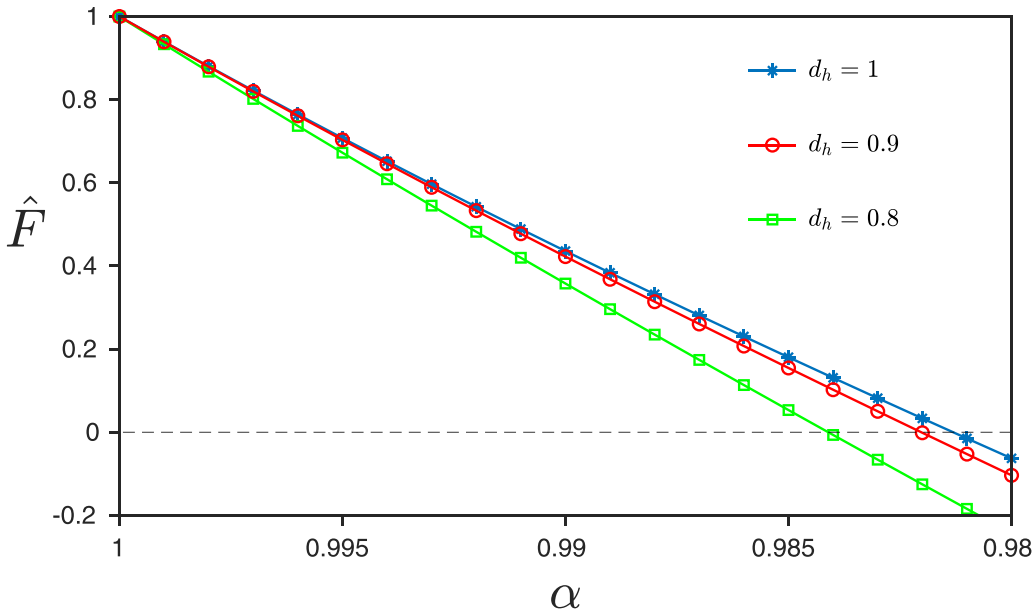

FIG. 4. Analytical stability curve for different predator dispersal rates. The values of the parameters are the same as in Fig. 3.

density is depicted in the bifurcation diagram as a function of the carrying capacity k (see Fig. 5). The prey and predator dispersal rates are fixed as $d_v = 0.001$ and $d_h = 1$, respectively. The dynamical states are the same as in Fig. 2. The trivial steady state loses its stability via a transcritical bifurcation at $k = k_{TB}$ leading to a nontrivial homogeneous steady state, which undergoes a supercritical Hopf bifurcation (HB1) resulting in stable homogeneous oscillation and an unstable steady state at $k = 0.4$ for $\alpha = 1$ [see Fig. 5(a)]. Using the standard linear stability analysis around the homogeneous steady state $(\frac{kr+kd_v(\beta-1)}{r}, 0, \frac{kr+kd_v(\beta-1)}{r}, 0)$, the transcritical bifurcation at $k = k_{TB}$ can be deduced as

$$k_{TB} = \frac{b(d_h + m - \alpha d_h)}{ac + d_h(\alpha - 1) - m}.$$

Similarly, one can obtain the Hopf bifurcation

$$k_{HB} = \frac{b[ac + m + (1 - \alpha)d_h]}{ac + (\alpha - 1)d_h - m}$$

by performing a linear stability analysis around the homogeneous steady state (V^*, H^*, V^*, H^*), where $V^* = \frac{bm+bd_h(1-\alpha)}{ac-m-d_h(1-\alpha)}$, $H^* = \frac{bc\{ack[r+d_v(\beta-1)]-[br+kr+kd_v(\beta-1)][m+d_h(1-\alpha)]\}}{k[ac-m+d_h(\alpha-1)]^2}$. Note that for $\beta = \alpha = 1$, the Hopf and pitchfork bifurcation points and curves can be reduced to those in Ref. [31]. The stable homogeneous oscillatory state prevails in the entire explored range of $k \in [0.4, 2]$. A subcritical Hopf bifurcation (HB2) emerges at $k = 0.458$ resulting in unstable inhomogeneous oscillations and stable inhomogeneous steady states in the range $k \in [0.458, 1.043)$ leading to the existence of alternative stable states of the metacommunity. The latter loses its stability via a supercritical Hopf bifurcation (HB3) at $k = 1.043$ resulting in stable inhomogeneous oscillations in the range $k \in [1.043, 1.226)$ and unstable inhomogeneous steady states in the range $k \in [1.043, 2.0]$, leaving behind the synchronized oscillatory states as the only stable states of the metacommunity A saddle-node bifurcation emerges at $k = 1.226$. In the following, we will unravel the effect of limited dispersal as a function of the carrying capacity.

The bifurcation diagram elucidating the dynamical transitions of the metacommunity for $\alpha = 0.95$ is depicted in Fig. 5(b). The dynamical states and their transitions are almost similar to that discussed in Fig. 5(a) for $\alpha = 1.0$. Nevertheless, it is evident from the figure that the spread of the stable inhomogeneous steady (asynchronous alternative states) states increased to a larger extent, thereby increasing the degree of persistence of the metacommunity. However, this tendency, enhancing the spread of stable inhomogeneous steady states, of the degree of the dispersal persists up to a critical value, and then the steady states lose their stability eventually resulting in the homogeneous (synchronous) oscillatory state as the only dynamical state as illustrated in Fig. 5(c) for $\alpha = 0.9$. The spread of the stable inhomogeneous steady states for different values of α is depicted in Fig. 6 as a function of the carrying capacity k. It is also evident from the figure that the degree of the spread of inhomogeneous steady states increases initially for a small decrease in the dispersal and eventually decreases for further decrease in the dispersal beyond a critical value of α. The spread of the homogeneous and inhomogeneous states is shown in Fig. 7 as two-parameter bifurcation diagrams in (k, d_h) parameter space for different degrees of the predator dispersal. The homogeneous state prevails in the entire parameter space, whereas the stable inhomogeneous steady states prevail only in the shaded regions leading to multistability. It is also evident from the figures that the spread of the stable inhomogeneous steady states increases for a small decrease in the degree of the predator dispersal up to a critical value of α, and then it starts decreasing as a function of α. The stable inhomogeneous steady states eventually destabilized from the entire parameter space, where it was stable, resulting in the homogeneous states as the only dynamical states of the metacommunity. Thus, the degree of limiting the predator dispersal results in increasing the persistence of the metacommuntiy

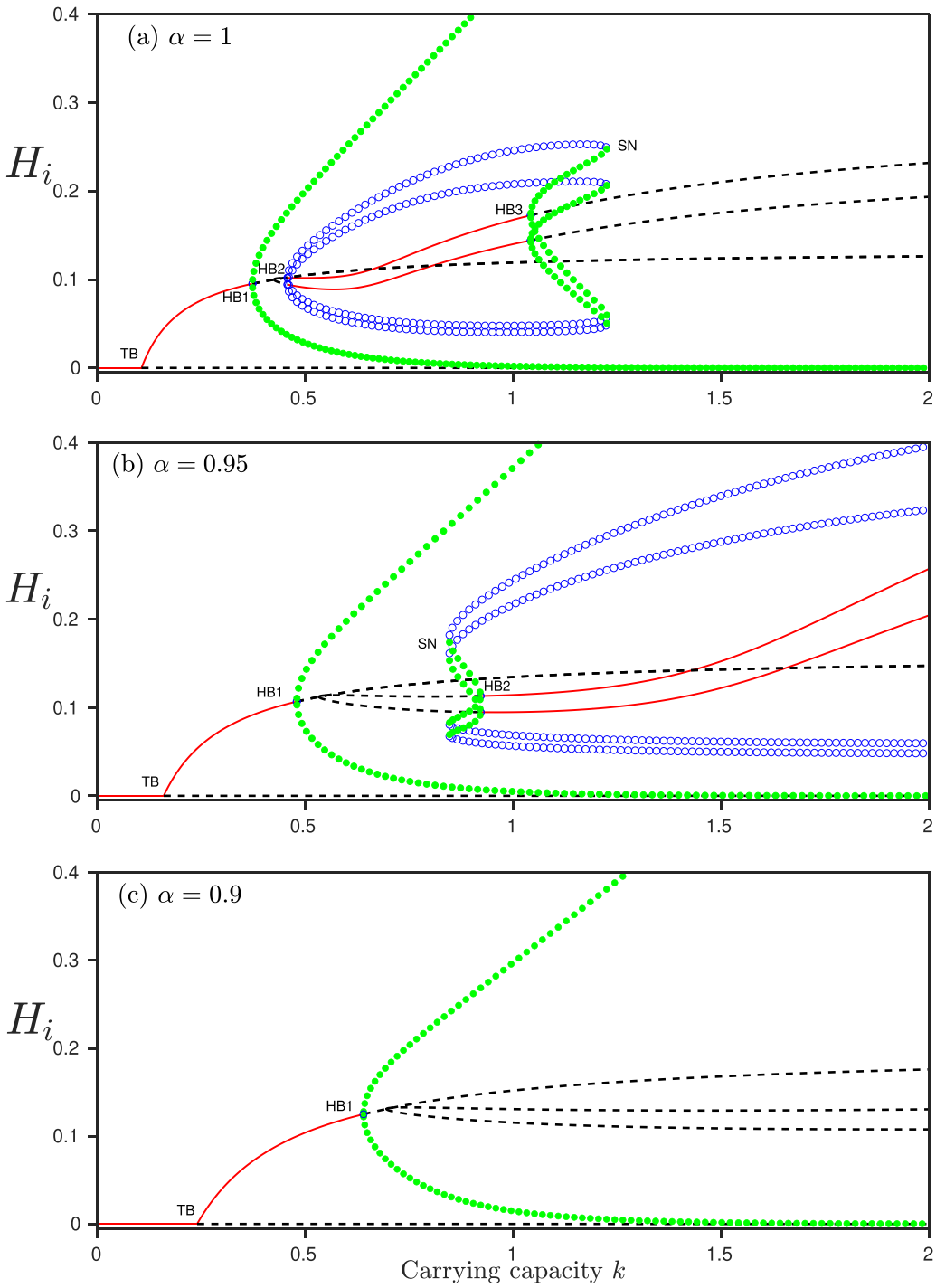

FIG. 5. Metacommunity dynamics for limiting the predator dispersal: Bifurcation diagram as a function of the carrying capacity (k) is shown for different α values. Homogeneous and inhomogeneous states of the metacommunity are shown for (a) $\alpha = 1$, (b) $\alpha = 0.95$, and (c) $\alpha = 0.9$. For a decrease in α, inhomogeneous stable steady states (red solid lines) become unstable. Here TB, HB, and SN correspond to transcritical bifurcation, Hopf bifurcation, and saddle-node bifurcation, respectively. Other parameters are $r = 0.5$, $a = 1$, $c = 0.5$, $b = 0.16$, $m = 0.2$, $d_v = 0.001$, and $d_h = 1$.

until a critical value, above which it is endangered by the presence of homogeneous (synchronous) states as the only dynamical states of the metacommunity.

C. Limiting prey dispersal

Now we will investigate the effect of limiting the prey dispersal on the metacommunity dynamics as a function of the spatial parameter. For complete dispersal of the predators, that is, for $\alpha = 1$, the effect of limiting the prey dispersal on the metacommunity dynamics can be seen only in a narrow range of the parameter space. Hence, we have fixed $\alpha = 0.985$ and depicted the two-parameter bifurcation diagram in the (d_h, d_v) parameter space, where the effect of limiting the prey dispersal is well pronounced, as evident from Fig. 8. A

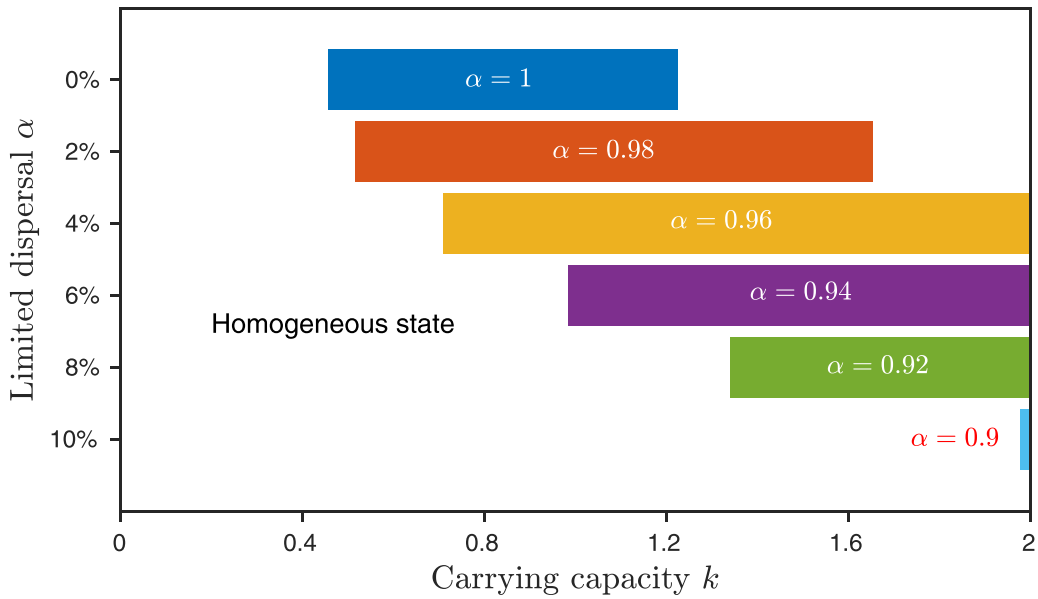

FIG. 6. Inhomogeneous states of the metacommunity for different α values: Each horizontal bar denotes the parameter range of k where the metacommunity exhibits inhomogeneous stable steady (asynchronous alternative) states. Other parameters are $\beta = 1$, $r = 0.5$, $a = 1$, $c = 0.5$, $b = 0.16$, $m = 0.2$, $d_v = 0.001$, and $d_h = 1$.

homogeneous oscillatory state is stable in the entire parameter space, while the inhomogeneous steady states are stable only in the shaded region. Transition from the homogeneous oscillatory state to inhomogeneous steady states is via the supercritical Hopf bifurcation (HB1) curve, which is obtained from XPPAUT. It is to be noted that for $\beta = 1$, that is, for uncontrolled prey dispersal, the spread of the inhomogeneous steady states is rather limited to smaller values of d_v. However, decreasing β, that is, limiting the prey dispersal, manifests the stable inhomogeneous steady states in a larger region of the (d_h, d_v) parameter space. For instance, the spread of the stable inhomogeneous steady states is depicted in Fig. 8 for $\beta = 0.7$ and 0.5. Thus, limiting the prey dispersal results in a large degree of the metacommunity persistence in contrast

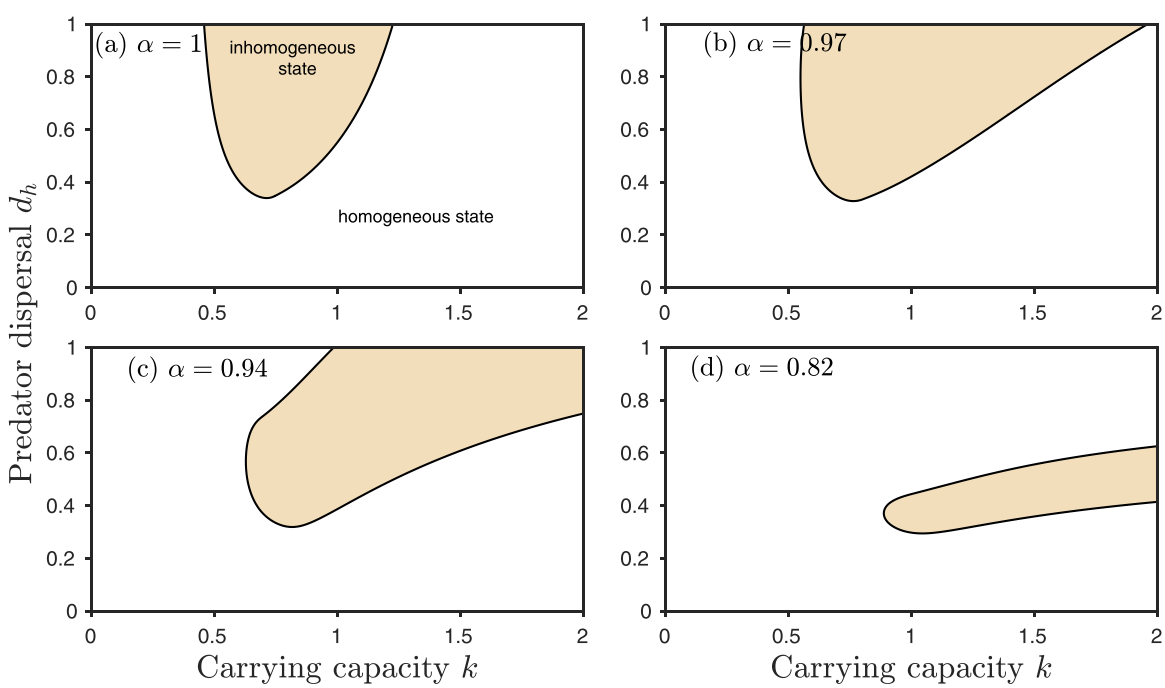

FIG. 7. Two-parameter bifurcation diagram in (k, d_h) parameter space for different α values. Here the shaded region indicates the parameter space where the metacommunity exhibits inhomogeneous stable states. Outside the shaded region, metacommunity exhibits only a homogeneous state. For decreasing α, inhomogeneous region is increased at first, and then decreased. Other parameters are $r = 0.5$, $\alpha = 1$, $\beta = 0.5$, $B = 0.16$, $m = 0.2$, and $d_v = 0.001$.

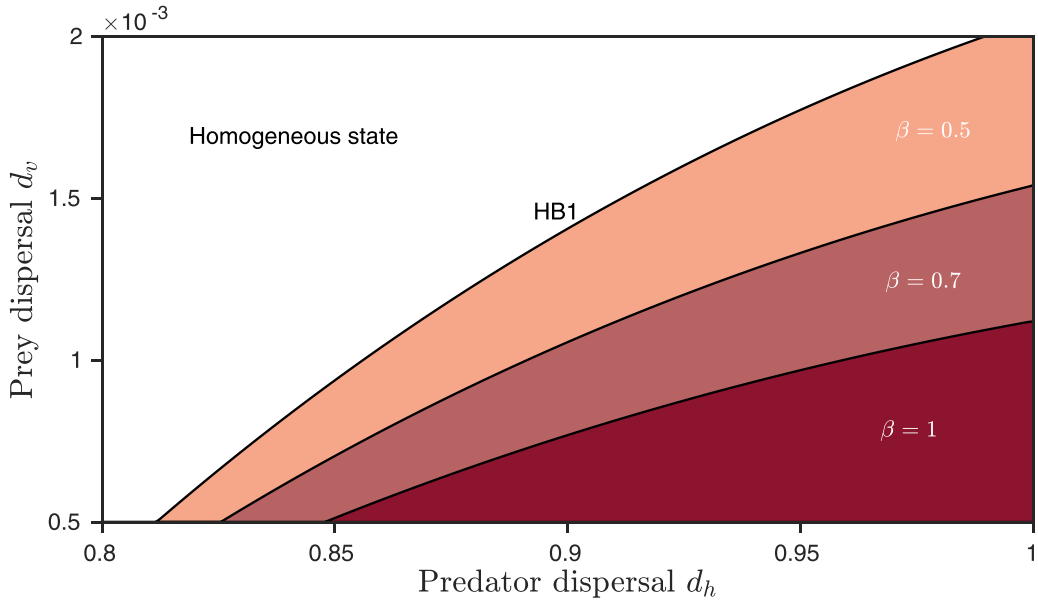

FIG. 8. Two-parameter bifurcation diagram in d_h-d_v space at different β values: the Hopf bifurcation (HB1) curve separates the region into homogeneous and inhomogeneous stable states. Other parameter values are $r = 0.5$, $k = 0.5$, $a = 1$, $c = 0.5$, $b = 0.16$, $m = 0.2$, and $\alpha = 0.985$.

to the effect of limiting the predator dispersal. It is also to be noted that for different degrees of local parameter (carrying capacity), limiting the prey dispersal results in an increase in the metacommunity persistence.

D. Limiting predator dispersal in a larger network

To elucidate the generic nature of our results, we consider an arbitrary network consisting of N patches, whose governing equation is represented as

$$\frac{dV_i}{dt} = rV_i\Big(1 - \frac{V_i}{k}\Big) - \frac{aV_i}{V_i + b}H_i + \frac{d_v}{d_j}\sum_{j=1}^{N} g_{ij}(\beta V_j - V_i), \tag{5a}$$

$$\frac{dH_i}{dt} = \frac{caV_i}{V_i + b}H_i - mH_i + \frac{d_h}{d_j}\sum_{j=1}^{N} g_{ij}(\alpha H_j - H_i), \tag{5b}$$

where $i = 1, \ldots, N$. g_{ij} encodes the topology of the underlying network. $g_{ij} = g_{ji} = 1$ if ith and jth oscillators are connected, otherwise $g_{ij} = g_{ji} = 0$. $d_j = \sum_{j=1}^{N} g_{ij}$ corresponds to the degree of the jth oscillator. The other parameters are the same as in Eq. (1). We have fixed the values of the parameters as $\beta = 1.0$, $r = 0.5$, $a = 1$, $c = 0.5$, $b = 0.16$, $m = 0.2$, $d_h = 1$ $k = 0.5$, and $d_v = 0.001$. Here we have fixed $N = 20$ patches. The dynamics of a random (Erdős-Rényi) network is depicted as spatiotemporal and time series plots in Fig. 9 for different degree of the predator dispersal. The network exhibits a ten-cluster state, corresponding to ten stable steady states, for $\alpha = 1$ as evident from the spatiotemporal and time series plots in Fig. 9(a). Nevertheless, decreasing the degree of dispersal to $\alpha = 0.99$ results in an increase in the number of clusters [see Fig. 9(b)]. Note that the multicluster state corresponds to the alternative states of the metacommunity elucidating a high degree of their persistence. However, further decrease in the degree of the dispersal decreases the number of multicluster and eventually manifests as a single-cluster state, as depicted in Fig. 9(c) for $\alpha = 0.9$, at a critical value of α signaling a low degree of the metacommunity persistence.

The number of clusters is depicted as a function of the limiting factor α in Fig. 10(a) for the same values of the parameters as in Fig. 9. The size of the multicluster states initially varies for small decrease in the limiting factor and eventually decreases resulting in a single-cluster state (homogeneous state) at a critical value of $\alpha = \alpha_c = 0.907$. Thus, it is evident that the observed results of the two-patch metacommunity hold for a random network of metacommunity thereby corroborating the generic nature of the results.

Next denote ρ_j $(j = 1, 2, \ldots, N)$ as the eigenvalues of the connectivity matrix g_{ij}, characterizing an arbitrary network, which can be ordered as $1.0 = \rho_1 \geqslant \rho_2 \geqslant \cdots \geqslant -1/(N-1) \geqslant \rho_N \geqslant -1.0$ [33]. The smallest bounding eigenvalue of the connectivity matrix g_{ij} corresponding to the random network employed in Figs. 9 and 10(a) is found to be $\rho_N = -0.987$. It is known that the role of coupling topology on the stability of the homogeneous steady state is determined by ρ_N [34,35], which completely characterizes the effect of the connection topology corresponding to an arbitrary network. We have depicted the critical value of the limiting factor α_c as a function of ρ_N [36] in Fig. 10(b), which elucidates that our results are generic to any arbitrary network. Note that the entire range of $\rho_N \in [-1, 0]$ captures all possible coupling topologies. It is to be noted that limiting the prey dispersal rate always results in multicluster states (an inhomogeneous steady state) promoting metacommunity persistence, and hence the above analysis of calculating α_c cannot be applied to this case.

Further, different networks can be constructed for the same probability of rewiring p from complex networks perspective.

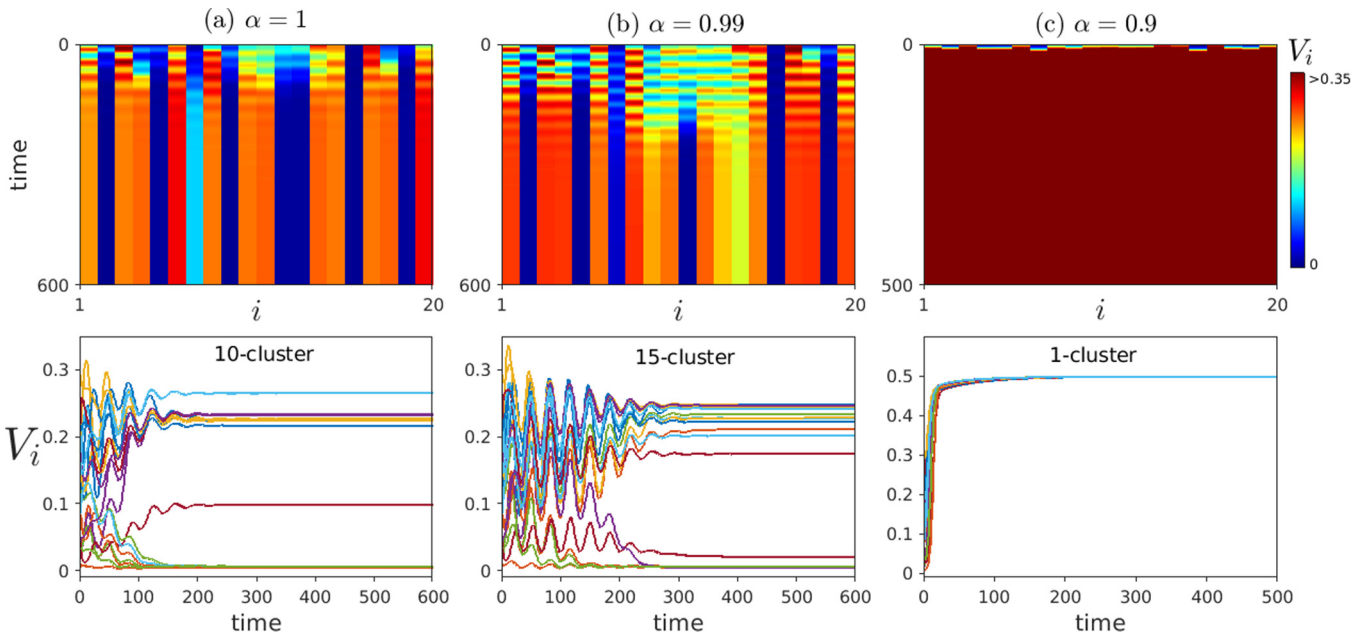

FIG. 9. Spatiotemporal dynamics of a random (Erdős-Rényi) network consisting of 20 patches: Top panel shows the spatial dynamics of the metacommunity, whereas the bottom panel shows the respective time series. The metacommunity shows dynamical transitions from 10 clusters to 15 clusters, which are further organized into a single cluster for decreasing degree of the limiting factor (α). Here initial conditions are the same for each α value. Other parameters are fixed as $\beta = 1$, $r = 0.5$, $a = 1$, $c = 0.5$, $b = 0.16$, $m = 0.2$, and $d_v = 0.001$.

Noted that the range of $p \in [0, 1]$ covers the entire class of network topologies from regular, small world to random (scale-free) networks [37]. The critical value of α is depicted in Fig. 11 as a function of p with error bars characterizing the effect of various network sizes N. Specifically, we have chosen $N = 20$ to 500 in steps of 10. The mean of all the critical values of the limiting factor corresponding to each N is indicated by the filled circle for each p, while their variance is denoted by the error bars. The inset in Fig. 11 clearly depicts the error bars. The critical value of the limiting factor in the entire range of p again corroborates the generic nature of our results.

IV. DISCUSSION

In this study, we have addressed how limiting both predator and prey dispersal of a spatially distributed community affects its stability and persistence. Using the homogeneous (synchronized) and inhomogeneous (asynchronized) dynamical states of a diffusively coupled predator-prey metacommunity, we have elucidated the importance of controlled dispersal at local and spatial scales. At spatial scale, a small decrease in the predator immigration through the limiting factor reduces the metacommunity persistence by inducing the homogeneous state. On the other hand, at local scale, metacommunity persistence is increased for a small decrease in the predator immigration up to a critical value and then decreases for further increase in the degree of the limited predator dispersal. Moreover, our findings reveal that there exists a critical value for the limiting factor, below which metacommunity persists and above which metacommunity goes to a high-risk state. However, limiting the prey dispersal promotes inhomogeneous steady states in a large region of the parameter space, thereby increasing the metacommunity persistence at both spatial and local scales. Further, we have showed the similar qualitative dynamics for an entire class of complex networks consisting of a large number of patches illustrating the robustness of our results, which remains unaltered in a large range of model parameters. Thus, our findings reveal that dispersal-dependent responses strongly influence the metacommunity persistence. Note that the spread of homogeneous and inhomogeneous steady states in the one-parameter bifurcation diagrams and two phase diagrams get rescaled only for the rescaled model (2).

Dispersal is a fundamental process for structuring natural ecosystems, and it is widely recognized in conservation and ecosystem management [3,11]. Since dispersal can rescue local populations from complete extinction, it is an important stabilizing mechanism for various ecological communities. However, dispersal induces synchrony among spatially connected populations which can elevate a high risk of extinction as compared to asynchronized dynamics [4,6]. Hence, theoretical understanding of population synchrony controlled by dispersal has received significant attention. Numerous theoretical studies have addressed the factors and mechanisms of synchrony using various coupling strategies [7,9,29,38]. Our study reveals the synchronized and asynchronized dynamics of the metacommunity through a control on the diffusive dispersal. In particular, a decrease in the species immigration destabilizes the metacommunity through synchronized behavior. Dispersal stabilizes the metacommunity through a source-sink behavior whereby some patches have a high population abundance and others have a low population abundance [39]. Various inhomogeneous dynamical states shown in this study represent the source-sink behavior, which in turn influences the metacommunity persistence.

"Paradox of enrichment," referring to the existence of high-amplitude extinction-prone cycles due to increasing carrying

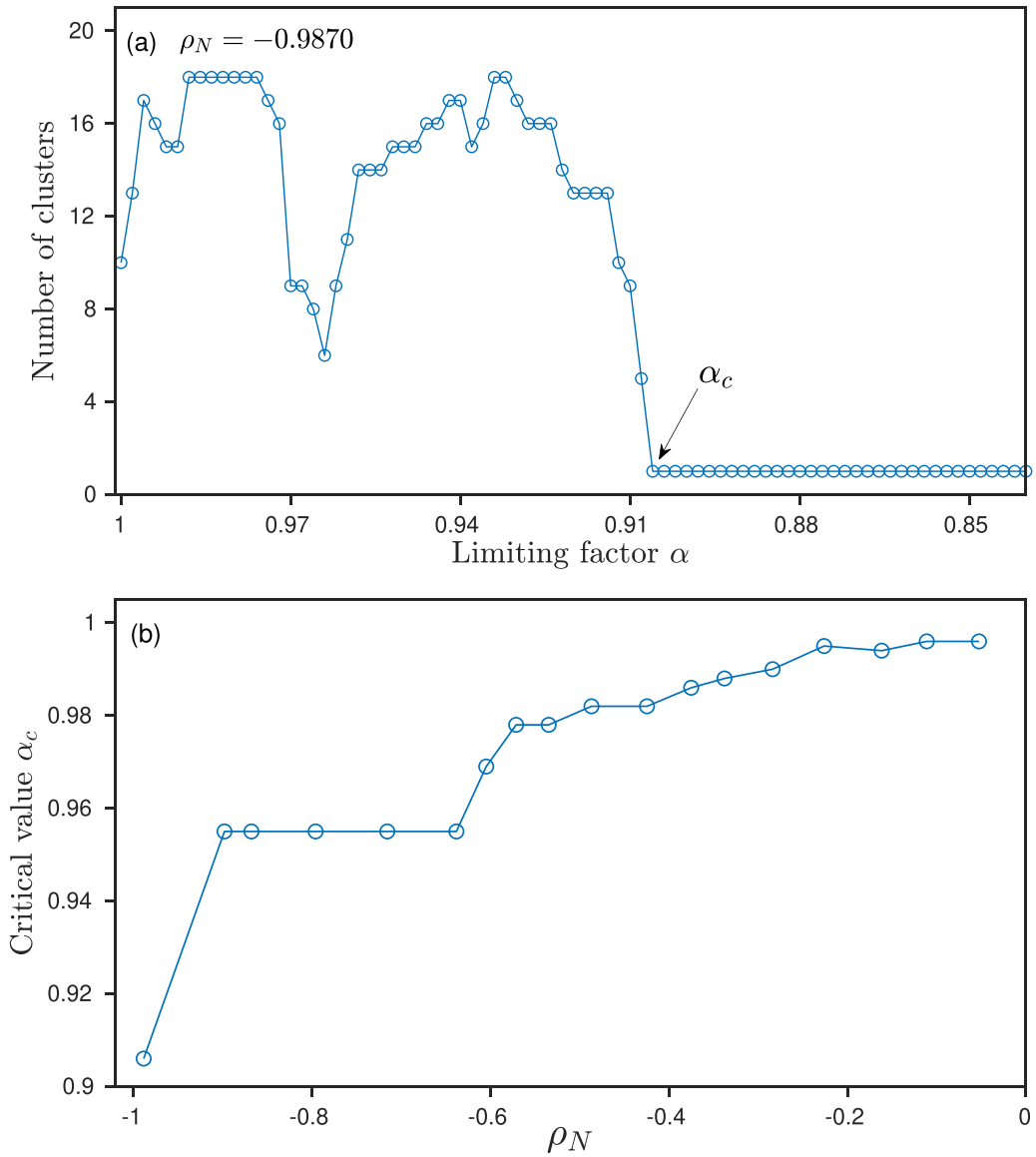

FIG. 10. (a) Number of clusters as a function of the limiting factor α for a random network of 20 nodes showing the transition from inhomogeneous steady states to homogeneous steady state, and (b) α_c as a function of the least bounding eigenvalue $\rho_N \in [-1, 0]$ of the connectivity matrix g_{ij}, characterizing the entire class of complex networks.

capacity, can destabilize the ecological community [40]. Our findings on varying carrying capacity with a controlled dispersal elucidated the solution to the "paradox of enrichment." In particular, our results are in line with previous studies that dispersal can prevent the extinction-prone cycles by creating inhomogeneous states and provide a solution to the paradox of enrichment [41–43]. In addition, our findings reveal that the inhomogeneous states can be manifested as homogeneous state by limiting the dispersal. Thus, limiting the dispersal offers insights to understand the stability and persistence of a spatially distributed community through synchronized and asynchronized dynamics.

In summary, this study presents the effect of limiting dispersal on metacommunity persistence at local and spatial scales. The dynamics that we observe may apply to other ecological scenarios such as environmental stochasticity, spatial heterogeneity, and higher tropical interactions (i.e., foodwebs). Since these ecological scenarios increase the complexity of systems, further investigation is required to understand how limiting the dispersal influences the stability of ecological communities. Overall, this study offers insights on the stability and persistence of spatially distributed ecological communities.

ACKNOWLEDGMENTS

S.R.C. and R.A. acknowledge IISER-TVM for the financial support. W.Z. acknowledges support from the National Natural Science Foundation of China (Grant No. 12075089) and the Natural Science Foundation of Guangdong Province, China (Grant No. 2019A1515011868). V.K.C. thanks DST, New Delhi for computational facilities under the DST-FIST program (SR/FST/PS-1/2020/135) to the Department of Physics. The work of V.K.C. is also supported by the

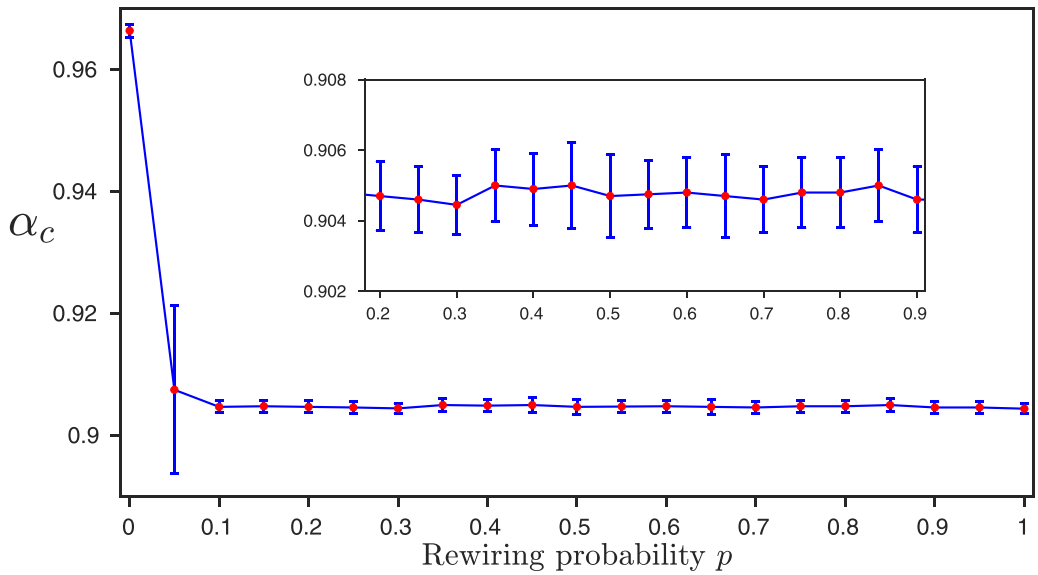

FIG. 11. The critical value of predator limiting factor α_c as a function of the probability of rewiring $p \in [0, 1]$ corresponding to the entire class of complex networks. The mean of all the critical values of the limiting factor corresponding to each N is indicated by the filled circle for each p, and their variance is denoted by the error bars. The inset in the specific range of p clearly depicts the error bars.

SERB-DST-MATRICS Grant No. MTR/2018/000676 and CSIR Project under Grant No. 03(1444)/18/EMR-II. D.V.S. is supported by the DST-SERB-CRG Project under Grant No. CRG/2021/000816.

[1] A. Pikovsky, M. Rosenblum, and J. Kurths, *Synchronization: A Universal Concept in Nonlinear Sciences*, Cambridge Nonlinear Science Series, Vol. 12 (Cambridge University Press, Cambridge, 2001).
[2] E. Izhikevich, *Dynamical Systems in Neuroscience* (MIT Press, Cambridge, MA, 2007).
[3] B. Blasius, A. Huppert, and L. Stone, Nature (London) **399**, 354 (1999).
[4] A. Liebhold, W. D. Koenig, and O. N. Bjørnstad, Annu. Rev. Ecol. Evol. Syst. **35**, 467 (2004).
[5] E. Ranta, V. Kaitala, J. Lindström, and H. Linden, Proc. R. Soc. London B **262**, 113 (1995).
[6] C. J. Briggs and M. F. Hoopes, Theor. Popul. Biol. **65**, 299 (2004).
[7] E. Goldwyn and A. Hastings, Theor. Popul. Biol. **73**, 395 (2008).
[8] E. Ranta, V. Kaitala, J. Lindström, and E. Helle, Oikos **78**, 136 (1997).
[9] B. E. Kendall, O. N. Bjørnstad, J. Bascompte, T. H. Keitt, and W. F. Fagan, Am. Nat. **155**, 628 (2000).
[10] M. Heino, V. Kaitala, E. Ranta, and J. Lindström, Proc. R. Soc. London B **264**, 481 (1997).
[11] M. D. Holland and A. Hastings, Nature (London) **456**, 792 (2008).
[12] M. Doebeli, Theor. Popul. Biol. **47**, 82 (1995).
[13] I. Hanski, Nature (London) **396**, 41 (1998).
[14] I. Hanski, *Metapopulation Ecology* (Oxford University Press, New York, 1999).
[15] S. Wang and M. Loreau, Ecol. Lett. **19**, 510 (2016).
[16] M. A. McPeek and R. D. Holt, Am. Nat. **140**, 1010 (1992).
[17] M. Doebeli and G. D. Ruxton, Evolution **51**, 1730 (1997).
[18] J. M. Travis, M. Delgado, G. Bocedi, M. Baguette, K. Bartoń, D. Bonte, I. Boulangeat, J. A. Hodgson, A. Kubisch, V. Penteriani *et al.*, Oikos **122**, 1532 (2013).
[19] K. E. Fussmann, F. Schwarzmüller, U. Brose, A. Jousset, and B. C. Rall, Nat. Clim. Change **4**, 206 (2014).
[20] G. R. Walther, E. Post, P. Convey, A. Menzel, C. Parmesan, T. J. Beebee, J. M. Fromentin, O. Hoegh-Guldberg, and F. Bairlein, Nature (London) **416**, 389 (2002).
[21] C. Parmesan, Annu. Rev. Ecol. Evol. Syst. **37**, 637 (2006).
[22] M. P. Berg, E. T. Kiers, G. Driessen, M. Van Der Heijden, B. W. Kooi, F. Kuenen, M. Liefting, H. A. Verhoef, and J. Ellers, Global Change Biol. **16**, 587 (2010).
[23] G.-R. Walther, Philos. Trans. R. Soc. B **365**, 2019 (2010).
[24] T. E. Reed, D. E. Schindler, and R. S. Waples, Conserv. Biol. **25**, 56 (2011).
[25] T. Mueller, R. B. O'Hara, S. J. Converse, R. P. Urbanek, and W. F. Fagan, Science **341**, 999 (2013).
[26] T. Püttker, A. A. Bueno, C. dos Santos de Barros, S. Sommer, and R. Pardini, PLoS ONE **6**, e27963 (2011).
[27] M. L. Rosenzweig and R. H. MacArthur, Am. Nat. **97**, 209 (1963).
[28] P. S. Dutta and T. Banerjee, Phys. Rev. E **92**, 042919 (2015).
[29] R. Arumugam, P. S. Dutta, and T. Banerjee, Phys. Rev. E **94**, 022206 (2016).
[30] R. Arumugam and P. S. Dutta, Phys. Rev. E **97**, 062217 (2018).
[31] R. Arumugam, V. K. Chandrasekar, and D. V. Senthilkumar, Phys. Rev. E **104**, 024202 (2021).
[32] B. Ermentrout, *Simulating, Analyzing, and Animating Dynamical Systems* (Society for Industrial and Applied Mathematics, Philadelphia, 2002).
[33] F. M. Atay, J. Diff. Equ. **221**, 190 (2006).

[34] W. Zou, D. V. Senthilkumar, M. Zhan, and J. Kurths, Phys. Rev. Lett. **111**, 014101 (2013).
[35] W. Zou, D. V. Senthilkumar, M. Zhan, and J. Kurths, Phys. Rep. **931**, 1 (2021).
[36] A connectivity matrix characterized by $\rho_N \in (-1, 0)$ can be obtained using the Watts-Strogaz algorithm with a certain probability of rewiring of a regular network.
[37] D. J. Watts and S. H. Strogatz, Nature (London) **393**, 440 (1998).
[38] J. Ripa, Oikos **89**, 175 (2000).
[39] P. C. Dias, Trends Ecol. Evol. **11**, 326 (1996).
[40] M. L. Rosenzweig, Science **171**, 385 (1971).
[41] V. A. A. Jansen, Oikos **74**, 384 (1995).
[42] C. Hauzy, G. Nadin, E. Canard, I. Gounand, N. Mouquet, and B. Ebenman, PLoS ONE **8**, e82969 (2013).
[43] I. Gounand, N. Mouquet, E. Canard, F. Guichard, C. Hauzy, and D. Gravel, Am. Nat. **184**, 752 (2014).